European Journal of Medicinal Chemistry 90 (2015) 1–9

Contents lists available at ScienceDirect

European Journal of Medicinal Chemistry

journal homepage: http://www.elsevier.com/locate/ejmech

Original article

Haloperidol metabolite II prodrug: Asymmetric synthesis and biological evaluation on rat C6 glioma cells

Piera Sozio [a, 1], Jole Fiorito [b, 1], Viviana Di Giacomo [a, 1], Antonio Di Stefano [a], Lisa Marinelli [a], Ivana Cacciatore [a], Amelia Cataldi [a], Stephanie Pacella [a], Hasan Turkez [c], Carmela Parenti [d], Antonio Rescifina [d], Agostino Marrazzo [d, *]

[a] Dipartimento di Farmacia, Università degli Studi di Chieti Gabriele D'Annunzio, Via dei Vestini 31, 66100 Chieti, Italy
[b] Department of Pathology and Cell Biology and Taub Institute for Research on Alzheimer's Disease and the Aging Brain, Columbia University, 630 W 168th St., New York, NY 10032, USA
[c] Department of Molecular Biology and Genetics, Faculty of Science, Erzurum Technical University, 25240 Erzurum, Turkey
[d] Dipartimento di Scienze del Farmaco, Università degli Studi di Catania, Viale Andrea Doria 6, 95125 Catania, Italy

ARTICLE INFO

Article history:
Received 1 February 2014
Received in revised form
4 November 2014
Accepted 5 November 2014
Available online 6 November 2014

Keywords:
Glioma
HDAC
Sigma receptors
Inhibitors
Medicinal chemistry

ABSTRACT

In a previous work we reported the antiproliferative effects of (±)-MRJF4, a novel haloperidol metabolite II (HP-mII) (a sigma-1 antagonist and sigma-2 agonist) prodrug, obtained through conjugation to 4-phenylbutyric acid (PhBA) [a histone deacetylase inhibitor (HDACi)] via an ester bond. As a continuation of this work, here we report the asymmetric synthesis of compounds (*R*)-(+)-MRJF4 and (*S*)-(−)-MRJF4 and the evaluation of their biological activity on rat C6 glioma cells, derived from glioblastoma multiforme (GBM), which is the most common and deadliest central nervous system (CNS) invasive malignancy. Favourable physicochemical properties, high permeability in the parallel artificial membrane permeability assay (PAMPA), good enzymatic and chemical stability, in vivo anticancer activity, associated with the capacity to reduce cell viability and to increase cell death by apoptosis, render compound (*R*)-(+)-MRJF4 a promising candidate for the development of a useful therapeutic for gliomas therapy.

1. Introduction

Malignant gliomas are the most common types of primary brain tumours and remain one of the deadliest forms of brain cancer in humans. New efficient chemotherapeutics for such malignant gliomas treatment were developed over the years and many are still under investigation. There is evidence that the best treatment consists of surgical resection followed by chemotherapy; combination of prednisone, lomustine and vincristine could increase survival rate in children with gliomas, whereas temozolomide could prolong the survival of adult patients [1]. Despite the fact that different treatments are available, the prognosis remains poor, particularly for glioblastoma multiforme (GBM), which has survival rate of less than 3% at 3 years [2,3].

To date, new anticancer compounds that are currently in clinical trial for gliomas are inspired from existing molecules selected for other types of cancer. Mainly, these molecules target intracellular signalling pathways relative to either growth or angiogenesis and were efficient in preclinical models of gliomas [1]. Decreasing the level of migration in various cancer cell types, including GBM, commonly restores a certain level of sensitivity to apoptosis and/or cytotoxic drugs [4]. Furthermore, was reported that glioma cells tend to display an overexpression of sigma (σ) receptors [5]. In this regard, *N*-(1-benzylpiperidin-4-yl)-4-iodobenzamide (4-IBP), a selective σ_1 agonist, demonstrated significant anti-migratory in vitro activity in different analysed cancer cell lines, including the highly motile human U373-MG GBM cell line [4,6–8]. On the other hand, also haloperidol, a potent σ_1 antagonist used as anti-psychotic drug, showed antiproliferative effects against glioma cells at low concentration (5 μM) [9].

Literature data reported that the prodrug approach was widely used to improve the delivery of anticancer drugs (chlorambucil, camptothecin, paclitaxel, doxorubicin, and vinblastine) [10]. In our previous work, using this strategy, we synthesized (±)-MRJF4, a novel ester prodrug of haloperidol metabolite II (HP-mII) for the treatment of prostate cancer [10] (Fig. 1). HP-mII – endowed with σ_1 antagonist and σ_2 agonist properties – resulted to be more lipophilic than the parent drug following the esterification with

* Corresponding author.
E-mail address: marrazzo@unict.it (A. Marrazzo).
[1] These authors contribute equally to this work.

http://dx.doi.org/10.1016/j.ejmech.2014.11.012
0223-5234/

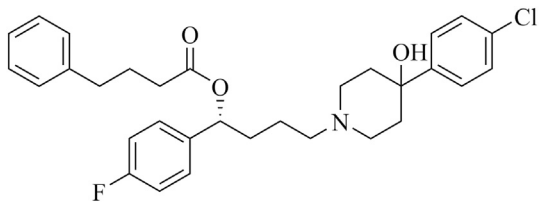

(*R*)-(+)-MRJF4

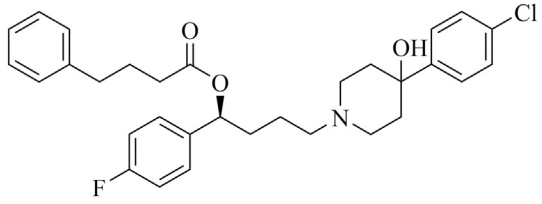

(*S*)-(−)-MRJF4

Fig. 1. Chemical structures of MRJF4 enantiomers.

PhBA (an HDACi) thus facilitating its entrance into CNS. MTT cell viability assays have highlighted a notable increase of antiproliferative activity of (±)-MRJF4 compared to PhBA, HP-mII, and respective equimolar pharmacological association. (±)-MRJF4 has also been used in combination with σ_1 agonist (+)-pentazocine and σ_2 antagonist AC927 to evaluate the role of σ receptor subtypes in prostate cancer cell death [11].

In this study we report the asymmetric synthesis of prodrugs (*R*)-(+)-MRJF4 and (*S*)-(−)-MRJF4 (Fig. 1) and the evaluation of their biological activity on rat C6 glioma cells, derived from GBM, which is the most common CNS invasive malignancy [12,13]. Taken into account that the blood brain barrier (BBB) restricts the delivery of systemically administered agents for treating brain tumours, we evaluated the pharmaceutical profiles of our new agents to determine their stability and the potential BBB permeability. Therefore, the present study included the evaluation of chemical and enzymatic stability of (*R*)-(+)-MRJF4 and (*S*)-(−)-MRJF4, their solubility in Fasted State Simulated Intestinal Fluid (FASSIF), and their respective permeability coefficient as measured by PAMPA assay.

Furthermore, we also investigated the effect of MRJF4 racemic mixture and its two enantiomers on the molecular mechanisms, which drive malignant C6 glioma cells proliferation and migration since gliomas constitute nearly 60% of primary brain tumours by inducing angiogenesis and infiltrating in the normal brain parenchyma. We also evaluated the ability of our prodrug ant its enantiomers to inhibit HDAC3, a member of HDACs upregulated in solid brain tumours; these prodrugs, being sensitive to esterases hydrolysis, can release PhBA, which is a well-known HDACi [14–16]. In fact, HDAC inhibitors (HDACis), alone or in combination with other drugs, are emerging as a new class of anticancer agents and were demonstrated to exert antitumour effects such as growth arrest, differentiation, and apoptosis [17,18].

2. Results and discussion

2.1. Chemistry

The synthesis of both enantiomers of the potential antineoplastic MRJF4 (4-[4-(4-chlorophenyl)-4-hydroxypiperidin-1-yl]-1-(4-fluorophenyl)butyl 4-phenylbutanoate) was achieved via the chiral reduction of 4-chloro-1-(4-fluorophenyl)-1-butanone (**1**) with (+)- or (−)-DIP-chloride, as also reported in literature [19], (Scheme 1). The obtained compounds (1*R*)-(+)-4-chloro-1-(4-fluorophenyl)butan-1-ol (*R*)-(+)-**2** and (1*S*)-(−)-4-chloro-1-(4-fluorophenyl)butan-1-ol (*S*)-(−)-**2** were condensed with 4-(4-methylphenyl)piperidin-4-ol, which is also reported in literature [19], and then esterified with 4-phenylbutanoyl chloride, according to the procedure already used by us [11], to give (*R*)-(+)-MRJF4 and (*S*)-(−)-MRJF4, respectively. All compounds were characterized by their ^{1}H and ^{13}C NMR spectroscopic data that resulted superimposable with the literature ones [11,19].

Moreover, the reduction of compound **1** resulted highly enantioselective and the target compounds (*R*)-(+)-MRJF4 and (*S*)-(−)-MRJF4 were isolated, after two recrystallization from ethyl acetate/diisopropyl ether, almost enantiomerically pure (98% ee and 99% ee, respectively) as ascertained by HPLC utilising a Chiralcel OJ[-RH] column (Fig. S1).

2.2. Biology

Major hurdle in the treatment of malignant glioma with systemic chemotherapy is the restricted delivery, due to the presence of BBB, of systemically administered agents for the therapy of brain tumours.

The physicochemical properties of drugs influence the diffusion through the biological membranes; therefore, their evaluation may be useful to understand the pharmacokinetics profile of drugs employed as antineoplastic agents in CNS tumours. Indeed, the apparent partition coefficient (log *P*) may be used to predict the distribution of a drug in a biological system and can be correlated to its adsorption, distribution, and CNS penetration. For both MRJF4 enantiomers water solubility and chemical stability were determined, while CLog*P* was theoretically calculated (Table 1); they displayed low water solubility (1.2 μg mL^{-1}) and relatively high lipophilicity values.

The chemical stability of (±)-MRJF4 was evaluated at pH 1.3 and pH 7.4 using a 0.02 M phosphate buffer, containing 0.1% (v/v) of Cremophor ELP at 37 °C (Table 2). The compounds showed good

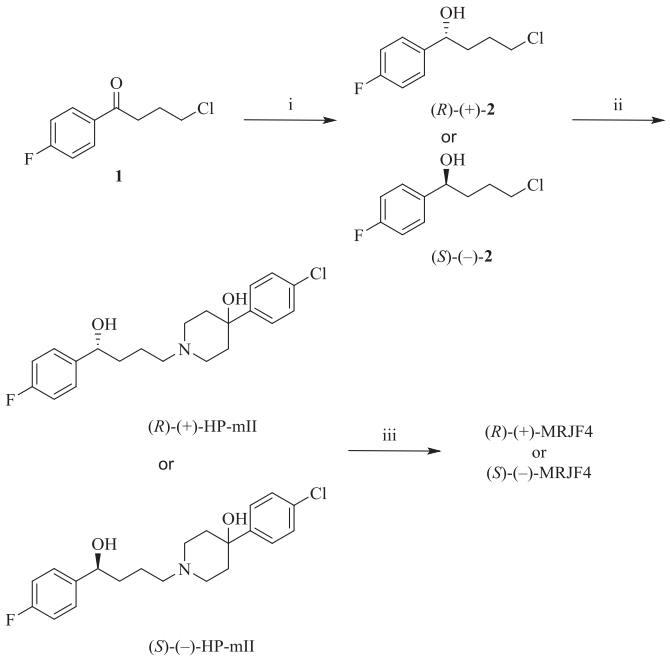

Scheme 1. Synthesis of MRJF4 enantiomers. (i) (+)-Ipc$_2$BCl or (−)-Ipc$_2$BCl, THF, 25 °C, $(HOCH_2CH_2)_2NH$, diethyl ether; (ii) 4-(4-methylphenyl)piperidin-4-ol, $NaHCO_3$, DMF, 80 °C; (iii) 4-phenylbutanoyl chloride, THF, DMAP, r.t.

Table 1
General characteristics of (±)-MRJF4 and its two enantiomers.

	(±)-MRJF4	(*R*)-(+)-MRJF4	(*S*)-(−)-MRJF4
Water solubility (μg/mL)[a]	1.2 ± 0.2	–	–
cLogP[b]	6.95 ± 0.45	–	–
PAMPA BBB P_{eff} (10^{-6} cm s^{-1})[c]	5.25	–	–

[a] Values are means SD of three experiments.
[b] *n*-Octanol/water partition coefficients were theoretically calculated by the program Clog*P* for windows, version 2.0 (Biobyte Corp., Claremont, CA), according to the methods based on the atom-additive and fragmental approaches.
[c] "CNS^+" (high BBB permeation predicted), $P_{eff} \geq 4.0 \times 10^{-6}$ cm s^{-1}; "CNS" (BBB uncertain permeation), P_{eff} from 4.0 to 2.0 × 10^{-6} cm s^{-1}; "CNS^-" (low BBB permeation predicted), $P_{eff} < 2.0 \times 10^{-6}$ cm s^{-1} [20,21].

Table 3
σ_1, σ_2, D_2 and D_3 binding assays.

Compound	K_i (nM) ± S.E.M.			
	σ_1	σ_2	D_2	D_3
(±)-MRJF4	162 ± 20[a]	105 ± 12[a]	>5000[a]	>5000[a]
(*R*)-(+)-MRJF4	87.5 ± 4.5	52.7 ± 3.8	>5000	>5000
(*S*)-(−)-MRJF4	230 ± 8.9	118 ± 7.3	>5000	>5000
(±)-HP-mII	2.3 ± 0.7[a]	2.0 ± 0.5	232 ± 46[a]	1095 ± 245[a]
(*R*)-(+)-HP-mII	2.0 ± 0.4	32.0 ± 2.0	256 ± 7.4	1278 ± 22
(*S*)-(−)-HP-mII	3.0 ± 0.8	9.8 ± 1.3	71.0 ± 3.5	353 ± 6.7
Haloperidol	2.5 ± 0.6	18.0 ± 2.2	2.3 ± 0.7	8.8 ± 1.5
DTG	70.1 ± 3.2	22.0 ± 3.5	n.d.[b]	n.d.[b]

[a] Ref. [11].
[b] Not determined.

stability both at pH 1.3 and 7.4 (about 5 days). The degradation products were not characterized.

The enzymatic stability of both MRJF4 enantiomers was also studied at 37 °C in rat and human plasma (Table 2). As could be deduced from the rate of hydrolysis (k_{obs}) both compounds undergo a fast hydrolysis in rat plasma, whereas in human plasma they were fairly stable. Taken together, these results point out that (*R*)-(+)- and (*S*)-(−)-MRJF4 are sufficiently stable in the acidic environment of the stomach and are potentially absorbed by the intestine after oral administration.

Moreover, to study the stability of (±)-MRJF4 in the presence of glioma C6 cells we adopted a mass spectrometric approach. Glioma C6 cells were incubated with (±)-MRJF4 (5 μM) for 24 h at 37 °C, and then the cell lysates were analysed [22] to verify the potential generation of metabolites within cells; in particular, a signal at *m*/*z* 214 was observed in the control cell lysates (Fig. S2, B). We identified additional prominent ions at *m*/*z* 524, 360, and 212 in the (±)-MRJF4-treated cell lysates (Fig. S2, C). The peak at *m*/*z* 524 refers to MRFJ4 (Fig. S2, A), while the peak at *m*/*z* 360 was generated from hydrolyses of ester bond followed by dehydration. We also identified a minor product ion at *m*/*z* 212 corresponding to 4-(4-chlorophenyl)-4-hydroxypiperidine. At 24 h after (±)-MRJF4 treatment, we observed two main peaks originated from hydrolysis of ester prodrug and one metabolite showing a reduced metabolism within the glioma C6 cells at physiological pH.

In order to better predict the ability of drugs to diffuse through the biological membranes, PAMPA was used as a non-cell-based assay for measuring passive permeability of the investigated compounds [23]. Depending on the phospholipid type, PAMPA can mimic different adsorption/permeation environments. In particular, porcine polar brain lipid is used for BBB permeation assays (PAMPA-BBB) [24]. Since our derivatives were not thoroughly soluble in the conventional buffer used for PAMPA, the permeability tests of new compounds were examined in the presence of co-solvents (0.1% (v/v) Cremophor ELP). To demonstrate that co-solvents do not change the permeability of the phospholipid layer at the investigated concentrations, we evaluated their effect on the permeability of Dopamine (DA), used as reference compound, due to its inability to cross the membrane passively. After 18 h of incubation, the effective permeability (P_{eff}) of DA was irrelevant, both in the presence and absence of co-solvents, indicating that the presence of Cremophor ELP did not alter the capacity of the phospholipid layer to act as a barrier [21].

Our results indicate that (±)-MRJF4 showed good permeability ($P_{eff} \geq 4 \times 10^{-6}$ cm s^{-1}) (Table 1) and, consequently, both (*R*)-(+)-MRJF4 and (*S*)-(−)-MRJF4 enantiomers seem to be very promising in BBB penetration [25,26].

Considering these results, binding affinity and selectivity were measured for both enantiomers of MRJF4 and HP-mII, by conducting competitive binding assays [11,27]. In the σ_1, σ_2, dopamine D_2 and D_3 assays, guinea pig membrane (for σ_1 and σ_2), rat striatum (for D_2), and rat olfactory tubercle (for D_3) tissue membranes were used as receptor sources. Moreover, [^{3}H]-(+)-pentazocine, [^{3}H]-1,3-di(2-tolyl)guanidine ([^{3}H]-DTG) with unlabelled (+)-pentazocine, [^{3}H]-spiperone and [^{3}H]-7-OH-DPAT were used as radioactive tracers.

Table 3 displays σ_1, σ_2, D_2, and D_3 receptor affinities of (+)-MRJF4, (−)-MRJF4, (+)-HP-mII, and (−)-HP-mII relative to respective racemic mixtures. The (+)- and (−)-enantiomers of HP-mII exhibited high σ_1 binding affinity (K_i = 2.0 ± 0.4 and 3.0 ± 0.8 nM, respectively). Moreover, (+)-HP-mII showed lower affinity to σ_2 receptor (K_i = 32.0 ± 2.0 nM) if compared with its opposite isomer (−)-HP-mII (K_i = 9.8 ± 1.3 nM) and haloperidol (K_i = 18.0 ± 2.2 nM), these data are in accord to literature ones [28]. The apparently anomalous higher affinity of (±)-HP-mII, for σ_2 receptors, with respect to its enantiomers, could be related to a positive allosteric modulation of the two enantiomers, as previously reported in literature for sigma receptors [29–33]. Conversely to haloperidol, (+)-HP-mII and (−)-HP-mII showed a reduced affinity for dopamine D_2 and D_3 receptors. In particular, (+)-HP-mII displayed a 111-fold lower affinity and a 145-fold lower affinity for D_2 and D_3 receptors (K_i − D_2 = 256 ± 7.4 nM; K_i − D_3 = 1278 ± 22 nM) with respect to haloperidol ($K_i - D_2 = 2.3 \pm 0.7$ nM; $K_i - D_3 = 8.8 \pm 1.5$ nM), while (−)-HP-mII displayed a K_i value of 71.0 ± 3.5 nM and 353 ± 6.7 nM for D_2 and D_3 receptors, respectively. According to our previously reported data on (±)-MRJF4 [11], the esterification of the hydroxyl group on the (+)- and (−)-HP-mII enantiomers with PhBA decreased the affinity

Table 2
Chemical and enzymatic stabilities of (±)-MRJF4 and its two enantiomers.

Stability		(±)-MRJF4		(*R*)-(+)-MRJF4		(*S*)-(−)-MRJF4	
		$t_{½}$ (h)	k_{obs} (h^{-1})	$t_{½}$ (h)	k_{obs} (h^{-1})	$t_{½}$ (h)	k_{obs} (h^{-1})
Chemical[a]	pH 1.3	140.1 ± 4.2	0.005 ± 0.001	–	–	–	–
	pH 7.4	127.2 ± 2.5	0.005 ± 0.001	–	–	–	–
Enzymatic[a]	Rat plasma	0.108 ± 0.004	6.41 ± 0.16	0.312 ± 0.004	2.22 ± 0.07	0.224 ± 0.002	3.09 ± 0.09
	Human plasma	92.0 ± 1.4	0.008 ± 0.001	84.3 ± 1.1	0.008 ± 0.001	90.7 ± 1.0	0.008 ± 0.001

[a] Values are means SD of three experiments.

for both σ receptor subtypes. Nevertheless, good σ_1 and σ_2 affinities were found in (+)-MRJF4 ($K_i - \sigma_1 = 87.5 \pm 4.5$ nM; $K_i - \sigma_2 = 52.7 \pm 3.8$ nM) compared to (−)-MRJF4 ($K_i - \sigma_1 = 230 \pm 8.9$ nM; $K_i - \sigma_2 = 118 \pm 7.3$ nM) and (±)-MRJF4 (Table 3). Compounds (+)-MRJF4 and (−)-MRJF4, analogously to racemate MRJF4, showed insignificantly affinity for dopamine D_2 and D_3 receptors ($K_i > 5000$ nM).

In the present study, we also investigated the effect of both enantiomers of MRJF4 on the molecular mechanisms of glioma cell migration and invasion. To assess the effects of (*R*)-(+)-MRJF4, (*S*)-(−)-MRJF4, and their racemic mixture on C6 cells, in terms of apoptosis and cell death, we performed flow cytometry analysis of Annexin-V/PI staining which allows the detection of apoptotic features by detecting phosphatidylserine exposure at the membrane level. Under treatment conditions, the amounts of Annexin V^{pos}/PI^{pos} late apoptotic cells and Annexin V^{neg}/PI^{pos} necrotic ones were significantly increased by (±)-MRJF4 and both enantiomers (Fig. 2); this increase was more significant after 48 h of treatment compared to 24 and 72 h samples. In particular, (*R*)-(+)-MRJF4 was the most effective compound (about 40% of late/necro) followed by (±)-MRJF4 and (*S*)-(−)-MRJF4 (35% and 25%, respectively).

The effect of all five compounds on C6 cell proliferation was studied after 24, 48, and 72 h of treatment at different concentrations ranging from 0 to 5 μM as time and dose response experiment (Fig. 3). Cell proliferation was inhibited in a concentration-

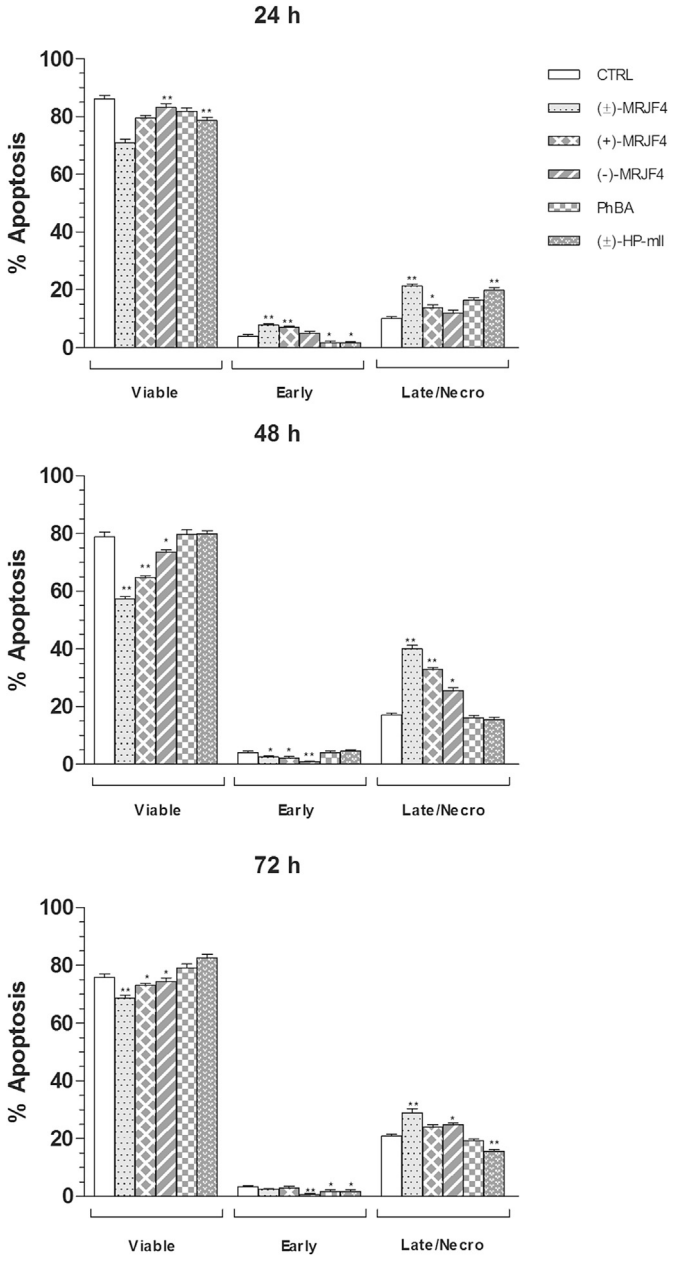

Fig. 2. Annexin V/PI detection of early apoptotic and apoptotic necrotic/late cells in C6 cells treated with 5 μM compounds (±)-MRJF4, (*R*)-(+)-MRJF4, (*S*)-(−)-MRJF4, PhBA and (±)-HP-mII for 24, 48, and 72 h. Early apoptotic cell populations (Annexin-V^{pos}/PI^{neg}) can be discriminated from late apoptotic (Annexin-V^{pos}/PI^{pos})/necrotic cells (AnnexinV^{neg}/PI^{pos}) according to their fluorescence emission. $^{*}p < 0.05$; $^{**}p < 0.01$ relative to control sample.

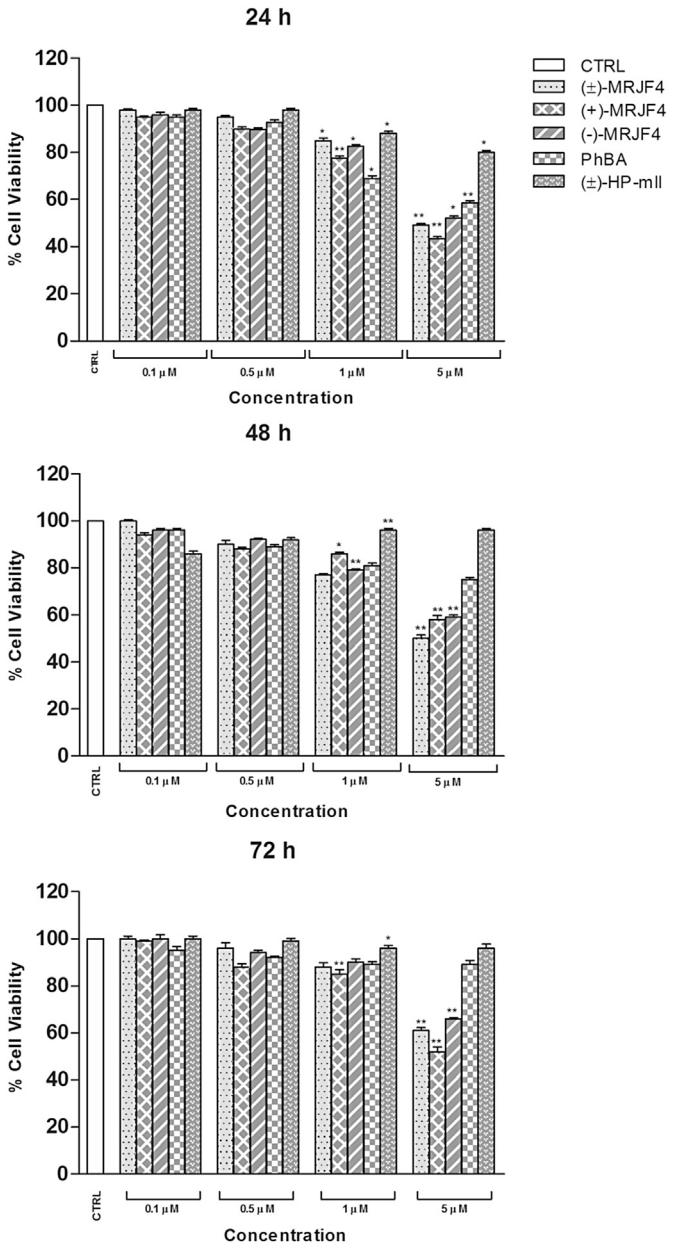

Fig. 3. Effects of compounds (±)-MRJF4, (*R*)-(+)-MRJF4, (*S*)-(−)-MRJF4, PhBA and (±)-HP-mII on C6 cell proliferation. Graphs show results of MTT assay after 24, 48, and 72 h of treatment with increasing concentration of all five agents. $^{*}p < 0.05$; $^{**}p < 0.01$ relative to control sample.

dependent manner. At 24 h, concentrations higher than 0.5 μM induced a significant reduction of cell viability in all treated samples, with (*R*)-(+)-MRJF4 being the most effective (40% of the control sample with respect to about 50% of (*S*)-(−)-MRJF4 and of (±)-MRJF4) with IC_{50} value of 5 μM. At 48 h, the samples treated with (±)-HP-mII did not show any significant decrease of cell viability; PhBA reduced cell viability of about 20%, while the cell viability of samples treated with the other three compounds was around 60%. At 72 h, only (±)-MRJF4, (*R*)-(+)-MRJF4, and (*S*)-(−)-MRJF4 retained an antiproliferative effect with cell viability decrease of about 40%.

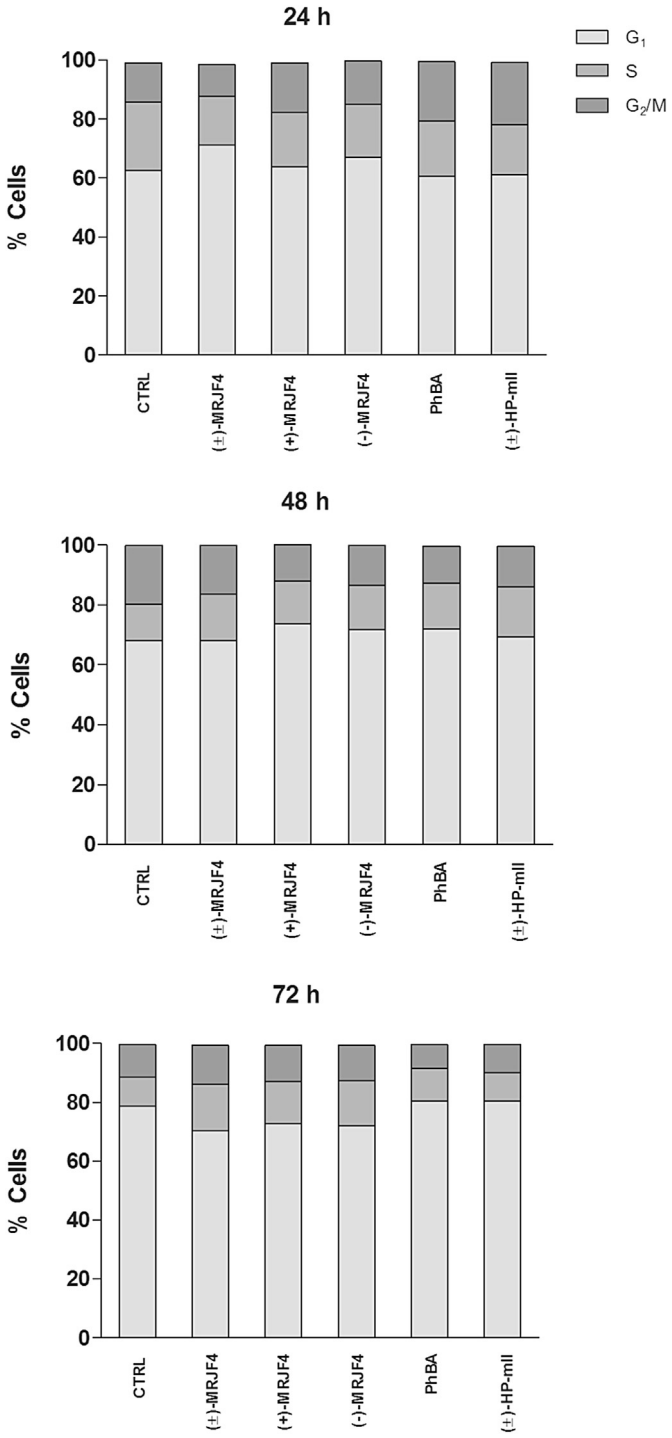

Fig. 4. Effects of a 5 μM concentration of compounds (±)-MRJF4, (*R*)-(+)-MRJF4, (*S*)-(−)-MRJF4, PhBA, and (±)-HP-mII on cell cycle progression of C6 cells. The amount of cells in G_1, *S*, and G_2/M phase can be detected correlating the number of events with the fluorescence emission on FL3. Graphs show the percentage of cells found in G_1, *S* and G_2/M phase.

Since (±)-MRJF4 causes a notable increase of antiproliferative activity in LNCaP and PC3 cell lines [11], flow cytometry cell cycle analysis on C6 cells was performed. Our analysis showed an increase in the S phase when cells were treated with (±)-MRJF4 and both enantiomers for 72 h (Fig. 4), whereas shorter treatments did not produce any significant changes. Such effects were quite evident in the histograms events/DNA content of 72 h that showed an increased S phase with (±)-MRJF4 and both enantiomers, while in samples treated with PhBA and (±)-HP-mII S phase was found comparable to controls.

Transwell chamber assay was employed to determine the effect of these agents on the migration capability of C6 glioma cell line. As shown in Fig. 5, the percentage of cells passing through the inserted filter significantly decreased when cells were treated for 24 h with compound (±)-MRJF4 and both enantiomers (less than 10% *vs* almost 60% in the control sample). On the other hand, PhBA and (±)-HP-mII had no effect on the capability of C6 glioma cell migration.

To evaluate the inhibitory activity of our compounds, histone3 (H3) acetylation was also investigated at 6, 15, and 24 h after treatment (Fig. 6). After 6 h the inhibition was especially augmented by (*R*)-(+)-MRJF4 (16.1% *vs* 4.5% of the DMSO); (±)-MRJF4 had the same activity as PhBA (about 14%) while the other compounds did not produce any significant effects on acetylation. After 15 h of treatment, there were no changes in all samples with respect to the vehicle alone, whereas after 24 h (*R*)-(+)-MRJF4 showed an increase in H3 acetylation (7.2 *vs* 4.5 of the control sample); this effect could probably be due to the metabolic pathways involving both enantiomers. Specifically, first hydrolysis of ester generates HP-mII and the PhBA responsible for acetylation of H3 at 6 h. Subsequently, as already reported in literature, HP-mII could undergo additional metabolism generating 4-(*p*-fluorophenyl)-4-hydroxybutyric acid and/or haloperidol metabolite III able to interfere with HDAC activity only after 24 h [22,34,35].

3. Conclusions

Glioma is an aggressive cancer characterized by high mortality, especially in children. It is known that glioma cells tend to display an overexpression of σ receptors. This study was aimed to explore the potential effects of haloperidol metabolite II prodrugs as useful

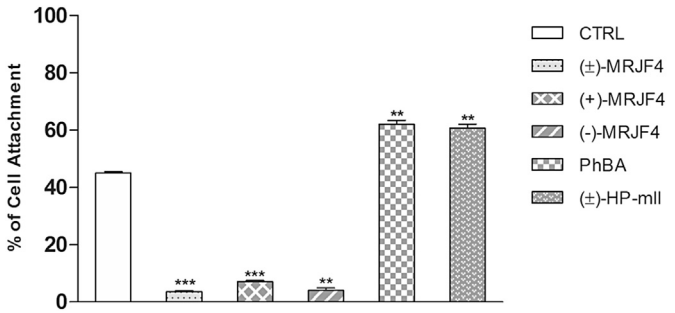

Fig. 5. Effects of a 5 μM concentration of compounds (±)-MRJF4, (*R*)-(+)-MRJF4, (*S*)-(−)-MRJF4, PhBA and (±)-HP-mII on C6 cell migration after 24 h. $^{*}p < 0.05$; $^{**}p < 0.01$; $^{***}p < 0.001$ relative to control sample.

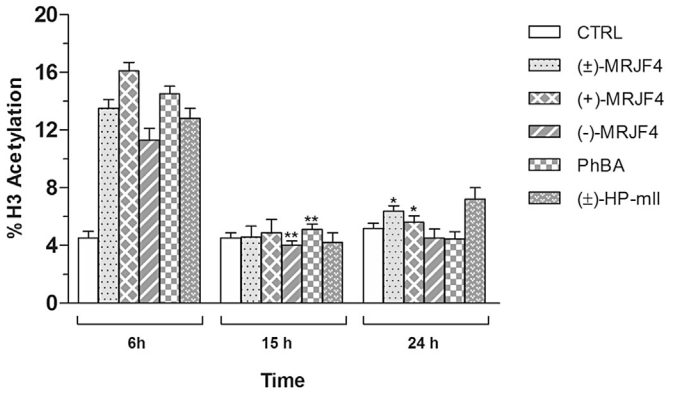

Fig. 6. Effects of a 5 μM concentration of compounds (±)-MRJF4, (*R*)-(+)-MRJF4, (*S*)-(−)-MRJF4, PhBA and (±)-HP-mII on H3 acetylation in C6 cells. Graph shows the percentage of acetylated H3. $^{*}p < 0.05$; $^{**}p < 0.01$ relative to control sample.

therapeutic tools for gliomas therapy. Taken together our results indicate that the racemic mixture and the two enantiomers exhibit good anticancer activity; they are able to reduce cell viability (measured by MTT assay), and to increase cell death by apoptosis. The obtained data indicate that cell proliferation is inhibited in concentration- but not in a time-dependent manner. The amounts of Annexin V^{pos}/PI^{pos} late apoptotic cells and Annexin V^{neg}/PI^{pos} necrotic ones were significantly increased with all compounds; in particular, results obtained with (*R*)-(+)-MRJF4 were more pronounced.

4. Experimental section

4.1. Material and methods

(+)- or (−)-DIP-chloride, 4-chloro-1-(4-fluorophenyl)-1-butanone, 4-(4-methylphenyl)piperidin-4-ol, and 4-phenylbutanoyl chloride were purchased from Sigma Aldrich (Milan, Italy). Cremophor® ELP was obtained from BASF-The chemical Company. All other chemicals were of the highest purity commercially available.

4.2. General

The identity of all new compounds was confirmed by NMR data. Homogeneity was confirmed by TLC on silica gel Merck 60 F_{254} and their purities (>98%) were quantified by HPLC and HR-MS. Solutions were routinely dried over anhydrous sodium sulphate prior to evaporation. Chromatographic purifications were performed by Merck 60 70–230 mesh ASTM silica gel column.

NMR spectra were recorded on a Varian VXR 300 MHz spectrometer. Chemical shifts are reported in parts per million (δ) downfield from the internal standard tetramethylsilane (Me_4Si). The LC-MS/MS system used consisted of an LCQ (Thermo Finnigan) ion trap mass spectrometer (San Jose, CA, USA) equipped with an electrospray ionization (ESI) source. The capillary temperature was set at 300 °C and the spray voltage at 4.25 kV. The fluid was nebulized using nitrogen (N_2) as both the sheath and the auxiliary gas. Melting points were determined on a Büchi B-450 apparatus and are uncorrected. Optical rotations were taken at 20 °C with a Perkin–Elmer 241 polarimeter. Microanalyses were performed on a EA1106 Carlo Erba CHN analyser; analyses indicated by the symbols of the elements or functions were within ±0.4% of the theoretical values.

Analytical HPLC measurements were run on a Waters 600 HPLC pump (Waters Corporation, Milford, MA, USA), equipped with a Waters 2996 photodiode array detector, a 20 μL Rheodyne injector and a computer-integrating apparatus. HPLC was performed using a Waters Symmetry RP-C18 column (150 × 4.6 mm, 5 μm); the mobile phase consisted in a mixture of acetonitrile, water, and formic acid. Two channels were used: channel A with acetonitrile/water 5/95 and 0.1% v/v of formic acid; channel B with acetonitrile and 0.1% v/v of formic acid. The gradient used was from 100% A to 100% B over 20 min, 100% B was maintained for 5 min and in the last minute, we came back to 100% of A. The flow rate was 1 mL min. The UV-detector was set at a length of 264 nm. Enantioselective HPLC analyses were carried out using the same above described apparatus and mobile phase utilising a Chiralcel OJ[-RH] column (150 × 4.6 mm, 5 μm).

4.3. Chemistry

4.3.1. (1R)-(+)- and (1S)-(−)-4-chloro-1-(4-fluorophenyl)-butan-1-ol, (R)-(+)-2 and (S)-(−)-2

Both compounds were synthesized as already reported in literature [19], and all analytical and spectral data are consistent with the reported ones.

4.3.2. (1R)-(+)- and (1S)-(−)-4-(4-chlorophenyl)-1-[4-(4-fluorophenyl)-4-hydroxybutyl]piperidin-4-ol, (R)-(+)-HP-mII and (S)-(−)-HP-mII

Both compounds were synthesized as already reported in literature [19], and all analytical and spectral data are consistent with the reported ones. Here we report only the data inherent to purity, obtained after two recrystallization from ethyl acetate/diisopropyl ether.

(*R*)-(+)-HP-mII, white solid, mp: 131–132 °C; 98% ee, $[\alpha]_D^{20} = +66.2$ ($c = 1.5$ in $CHCl_3$); HRMS-FAB: m/z $[M + H]^+$ calcd for $C_{21}H_{26}ClFNO_2$: 378.1636, found: 378.1633; Anal. calcd for $C_{21}H_{25}ClFNO_2$: (C, H, N, O).

(*S*)-(−)-HP-mII, white solid, mp: 132–133 °C; 99% ee, $[\alpha]_D^{20} = -67.7$ ($c = 1.5$ in $CHCl_3$); HRMS-FAB: m/z $[M + H]^+$ calcd for $C_{21}H_{26}ClFNO_2$: 378.1636, found: 378.1639; Anal. calcd for $C_{21}H_{25}ClFNO_2$: (C, H, N, O).

4.3.3. (1R)-(+)- and (1S)-(−)-4-[4-(4-chlorophenyl)-4-hydroxypiperidin-1-yl]-1-(4-fluorophenyl)butyl 4-phenylbutanoate, (+)-(R)-MRJF4 and (−)-(S)-MRJF4)

To a solution of (*R*)-(+)-HP-mII or (*S*)-(−)-HP-mII (400 mg, 1.058 mmol) in anhydrous THF (10 mL) 4-phenylbutanoyl chloride (181 μL, 1.095 mmol) was added at 0 °C and under stirring. The reaction was left for 24 h at r.t. under a nitrogen atmosphere. Subsequently, a $NaHCO_3$ saturated solution (20 mL) was added and the organic solvent was evaporated. After extraction with CH_2Cl_2 and purification by flash chromatography the final compound (*R*)-(+)- or (*S*)-(−)-MRJF4 was obtained as a colourless oil (250 mg 45%): $R_f = 0.33$ ($CHCl_3$/MeOH 95:5); ^{1}H NMR (300 MHz, $CDCl_3$): δ 7.37–6.92 (m, 13H, ArH), 5.67 (t, $J = 6$ Hz, 1H, CH), 3.65 (bs, 1H, OH) 2.70–2.66 (m, 2H, CH_2), 2.56–2.51 (m, 2H, CH_2), 2.35–2.24 (m, 6H, $3CH_2$), 2.06–1.60 (m, 10H, $5CH_2$); ^{13}C NMR (75 MHz, $CDCl_3$): δ 172.71 (s, 1C, CO), 159.86 (s, $J = 330.2$ Hz, 1C, Ar), 148.74 (s, 1C, Ar), 141.28 (s, 1C, Ar), 136.39 (s, 1C, Ar), 134.12 (s, $J = 21$ Hz, 1C, Ar), 128.44 (s, $J = 54$ Hz, 2C, Ar), 128.38 (s, 2C, Ar), 128.19 (s, 2C, Ar), 126.06 (s, 2C, Ar), 125.98 (s, 1C, Ar), 115.58 (s, $J = 38$ Hz, 2C, Ar), 75.08 (s, 1C, CH), 71.00 (s, 1C, C), 58.12 (s, 1C, CH_2), 49.36, (s, 2C, CH_2), 38.28 (s, 2C, CH_2), 35.03 (s, 1C, CH_2), 34.18 (s, 1C, CH_2), 33.81 (s, 1C, CH_2), 26.47 (s, 1C, CH_2), 22.90 (s, 1C, CH_2).

(*R*)-(+)-MRJF4, 97.98% ee, R_t 3.21 min, $[\alpha]_D^{20} = +65.4$ ($c = 1.2$ in $CHCl_3$); HRMS-FAB: m/z $[M + H]^+$ calcd for $C_{31}H_{36}ClFNO_3$:

524.2368, found: 524.2372; Anal. calcd for $C_{31}H_{35}ClFNO_3$: (C, H, N, O).

(*S*)-(−)-MRJF4, 98.89% ee, R_t 3.48 min, $[\alpha]_D^{20} = -66.9$ ($c = 1.2$ in $CHCl_3$); HRMS-FAB: *m/z* $[M + H]^+$ calcd for $C_{31}H_{36}ClFNO_3$: 524.2368, found: 524.2371; Anal. calcd for $C_{31}H_{35}ClFNO_3$: (C, H, N, O).

4.3.4. (*R*)-(+)-MRJF4 and (*S*)-(−)-MRJF4) oxalates

Both enantiomers were transformed into oxalate salts to best preserve them for biological tests. All spectral data are consistent with the reported ones for (±)-MRJF4 [11].

(*R*)-(+)-MRJF4 oxalate, white solid, mp: 111–113 °C; 98% ee, HRMS-FAB: *m/z* $[M + H]^+$ calcd for $C_{31}H_{36}ClFNO_3$: 524.2368, found: 524.2371; Anal. calcd for $C_{33}H_{37}ClFNO_7$: (C, H, N, O).

(*S*)-(−)-MRJF4 oxalate, white solid, mp: 112–114 °C; 99% ee, HRMS-FAB: *m/z* $[M + H]^+$ calcd for $C_{31}H_{36}ClFNO_3$: 524.2368, found: 524.2365; Anal. calcd for $C_{33}H_{37}ClFNO_7$: (C, H, N, O).

4.4. Kinetics of chemical hydrolysis

A 0.02 M phosphate buffer of pH 7.4 or a 0.02 M chloridric buffer of pH 1.3, containing 0.1% (v/v) Cremophor ELP, was used to evaluate chemical stability at physiological pH. Reaction was initiated by adding 1 mL of 10^{-4} M stock solution (in acetonitrile) of the compound to 10 mL of thermostated (37 ± 0.5 °C) aqueous buffer solution. At appropriate time intervals (for a total period of one week), samples of 20 μL were withdrawn and analysed by HPLC. Pseudo-first-order rate constants (k_{obs}) for the hydrolysis of the compounds were then calculated from the slopes of the linear plots of log (% residual compound) against time. The experiments were run in triplicate and the mean values of the rate constants were calculated [25,26].

4.5. Kinetics of enzymatic hydrolysis

Human and rat plasma were obtained by centrifugation of blood samples containing 0.3% citric acid at 3000 × *g* for 15–20 min. Plasma fractions (4 mL) were diluted with 0.02 m phosphate buffer (pH 7.4) to give a final volume of 5 mL (80% plasma). Incubation was performed at 37 ± 0.5 °C using a shaking water bath. The reaction was initiated by adding 200 μL of a stock solution of drug (1 mg/mL in acetonitrile) to 5 mL of preheated plasma. Aliquots (100 μL) were taken at various times and deproteinized by mixing with 200 μL of 0.01 M HCl in methanol. After centrifugation for 5 min at 5000 × g, 10 μL of the supernatant layer were analysed by chromatography as described above. The amounts of remaining intact compound were plotted as a function of incubation time [36].

4.6. Water solubility

Compounds (*R*)-(+)-MRJF4 and (*S*)-(−)-MRJF4 (50 mg) were placed in deionized water (1 mL), shaken at 25 °C for 1 h to ensure the solubility equilibrium and then centrifuged. The supernatant (20 μL) was analysed by HPLC [37].

4.7. Lipophilicity

n-Octanol/water partition coefficients were theoretically calculated by the program Clog*P* for windows, version 2.0 (Biobyte Corp., Claremont, CA), according to the methods based on the atom-additive and fragmental approaches.

4.8. Stability studies of MRJF4 in glioma C6 cells

Glioma C6 cell lysates (2 mg) were prepared for the LC-MS analysis as reported by Kim et al. [22]. The stability of MRJF4 in presence and in absence of glioma C6 cells (at 24 h) was assayed using a LCQ™ Deca XP Plus LC/MS^n spectrometer (Thermo Finnigan, San Jose, CA, USA). The potential at the nanospray needle was set at 4400 V. The orifice potential was 46 V, and the curtain gas was 15 psi (pound-force per square inch).

4.9. PAMPA method

The following protocol was applied to measure the P_{eff} through the artificial membrane to predict oral absorption and BBB permeation. The effective permeability of BBB was measured using phospholipid mixture from porcine polar brain lipid extract, composed by phosphatidylcholine (PC) 12.6%, phosphatidylethanolamine (PE) 33.1%, phosphatidylserine (PS) 18.5%, phosphatidylinositol (PI) 4.1%, phospatidic acid (PA) 0.8% and 30.9% of other compounds (purchased from Avantis Polar Lipids-Alabaster, AL). Each donor filtration plate well was carefully impregnated with 5 μL of this solution and, immediately after, 150 μL of phosphate buffer (pH 7.4/pH 6.5), containing 500 μM of each compound, and *i*PrOH 20% as co-solvent was added. Then the drug-filled donor plate was placed into the acceptor plate that was prefilled with the same buffer (300 μL) as acceptor solution. After plate lid was replaced, the resulting assembled donor-acceptor plates were incubated at r.t. for 18 h, following which drugs concentration in the acceptor and donor solutions were determined by HPLC [38].

Log P_{eff} can be calculated from the equation below:

$$\text{Log } P_{\text{eff}} = \left[\frac{V_D \times V_A}{(V_D + V_A) \times A \times t}\right] - \ln\left(1 - \frac{[\text{drug}]_{\text{acceptor}}}{[\text{drug}]_{\text{equilibrium}}}\right)$$

where P_{eff} is the effective permeability coefficient (cm s^{-1}), V_D is volume of donor compartment (0.15 cm^3) and V_A is volume of acceptor compartment (0.30 cm^3), A is effective filter area (0.28 cm^2), t is incubation time for the assay (s), $[\text{drug}]_{\text{acceptor}}$ is the concentration of the compound in the acceptor compartment at the completion of the assay, and $[\text{drug}]_{\text{equilibrium}}$ is the concentration of compound at theoretical equilibrium.

4.10. Receptor binding studies

The σ_1, σ_2, D_2 and D_3 receptor binding studies were performed according to literature [11,27]. Briefly, guinea pig brain membranes (500 μg protein) were incubated with 3 nM [^{3}H]-(+)-pentazocine (29 Ci/mM; (K_d) was 14 ± 0.3 nM, $n = 3$) and six concentrations of tested compounds or sigma ligands (from 10^{-5} to 10^{-10} M) in 1 mL of 50 mM Tris–HCl (pH 7.4). The reaction was performed for 150 min at 37 °C and terminated by filtering the solution through Whatman GF/B glass fibre filters which were presoaked for 1 h in a 0.5% poly(ethylenimine) solution. Filters were washed with ice-cold buffer (2 × 4 mL). Nonspecific binding was assessed in the presence of 10 μM of unlabelled haloperidol. σ_2 binding assays were made according to the following protocol: Guinea pig brain membranes (360 μg protein) were incubated with 3 nM [^{3}H]DTG (53.3 Ci/mM; K_d = 11 ± 0.8 nM; $n = 3$) and each test compound (from 10^{-5} to 10^{-10} M) in 0.5 mL of 50 mM Tris–HCl (pH 8.0) for 120 min at room temperature in the presence of 400 nM (+)-SKF10,047 to mask σ_1 sites. Nonspecific binding was evaluated with DTG (5 μM). Each sample was filtered through Whatman GF/B glass fibres filters, which were presoaked for 1 h in a 0.5%

poly(ethylenimine) solution, using a Millipore filter apparatus. Filters were washed twice with 4 mL of ice-cold buffer.

The rat striatum and rat olfactory tubercle were used for D_2 and D_3 receptors, respectively. Tissue preparations and binding assays were carried out according to Mennini et al. [39]. After incubation, the samples were filtered through Whatman GF/B or GF/C glass fibre filters, which were pre-soaked in a 0.5% poly(ethylenimine) solution, using a Millipore filter apparatus. The filters were washed twice with 4 mL of a suitable ice-cold buffer.

Radioactivity was counted in 4 mL of 'Ultima Gold MV' in a 1414 Winspectral PerkinElmer Wallac or Beckman LS6500 scintillation counter. Inhibition constants (K_i values) were calculated using the EBDA/LIGAND program purchased from Elsevier/Biosoft.

4.11. Cell culture

C6 rat glioma cell line was obtained from the American Type Collection (ATCC) and maintained in HAM'S F12 supplemented with 2 mM Glutamine, penicillin-streptomycin (100 μg mL^{-1}) and 10% FBS. Cells were grown at 37 °C in a humidified atmosphere of 5% CO_2.

4.12. Cell viability assay

Cell viability was measured by MTT (3[4,5-dimethylthiazol-2-yl]-2,5-diphenyl tetrazolium bromide) growth assay, according to manufacturer's instruction (Sigma Aldrich, St Louis, USA). In this assay the cell number was quantified by the amount of tetrazolium reduction in viable mitochondria. Cultured cells were incubated into 24-well plate at 5×10^4 cells/well and exposed to various concentrations of all the five agents (0.1–5 μM). After 24, 48, and 72 h cells were processed and the absorbance of each well was detected at 570 nm. Percentage of viable cells was calculated using the equation $A_s/A_0 \times 100$ where A_s is the absorbance value obtained for a sample containing cells in the presence of a given concentration of agent, and A_0 is the absorbance value of vehicle treated control. Four independent experiments were repeated under the same experimental conditions.

4.13. Annexin-V/PI detection of apoptotic and necrotic cells in flow cytometry

To assess apoptosis, a commercial Annexin-V-FITC/PI Kit (Bender Med System, Vienna, Austria) was used according to the manufacturer instructions. Briefly, 2.5×10^5 cells were gently resuspended in binding buffer and incubated for 10 min at room temperature in the dark with Annexin-V-FITC. Samples were then washed, supravitally stained with propidium iodide (PI) (5 μg mL^{-1}) and analysed on a FC500 flow cytometer with the FL1 and FL3 detector in a log mode using the CXP analysis software (Beckmann Coulter, FL, USA). For each sample, at least 10^4 events were collected. Viable cells were Annexin-V^{neg}/PI^{neg} (unlabelled), early apoptotic cells were Annexin-V^{pos}/PI^{neg}, late apoptotic and necrotic cells were Annexin-V^{pos}/PI^{pos} and Annexin-V^{neg}/PI^{pos}, respectively.

4.14. Cell cycle analysis

Approximately 3×10^5 cells per experimental condition were harvested, fixed in 70% (v/v) cold ethanol and kept at 4 °C overnight. Cells were then resuspended in 20 μg mL^{-1} PI and 100 μg mL^{-1} RNAse, final concentrations. Cell cycle profiles (10^4 cells) were analysed by a FC500 flow cytometer with the FL3 detector in a linear mode using the CXP software (Beckmann Coulter, FL, USA). A dual FL3-Area/FL3-Width graph was used for the exclusion of aneuploid cells and nuclei doublets from further analysis. PI fluorescence gathered at linear FL3 was used to measure DNA content.

4.15. Migration assay

Cell migration was assayed by means of a transwell chamber containing a polycarbonate insert with 8 μm pores placed between the upper and lower wells (Corning, NY, USA). Cells were cultured to 70–80% of confluency, and then starved for 24 h in serum free condition. C6 glioma cells were then trypsinized, centrifuged and resuspended in serum free HAM'S F12 at a concentration of 10^5 cells mL^{-1}. 100 μL of such suspension was added to the upper chamber of the transwell and 600 μL of HAM'S F12 with 5% FCS was added in the lower chamber. Compounds, at a final concentration of 5 μM, were added 2 h later in order to allow cells to adhere to membrane. After 24 h of incubation at 37 °C, cells on the upper side of the filter were removed with a cotton swab, while cells that migrated through the pores to the lower side of the membrane were fixed with absolute methanol and stained with DAPI. The filter was then cut out with a scalpel, mounted on a slide and nuclei were counted under a microscope in five random fields whose area were known.

To calculate migration, the total number of cells was determined counting and averaging the total number of cells in each of the random fields. The number obtained was divided by area of the microscope viewing field and multiplied by the entire area of the transwell insert. Percentage of migration was calculated by dividing the total number of cells by the number of cells seeded and multiplying this value by 100 to get percent.

4.16. Flow cytometry detection of acetylated histone H3

C6 cells were stained for acetylated H3 as previously described [40]. Briefly, after incubation, cell culture medium was removed and cells were fixed for 15 min in 1% *p*-formaldehyde on ice. Then cells were trypsinized and pellets were washed with 1 mL of PBS/BSA 1% and centrifuged at 130 g for 10 min at 4 °C. Cell was then permeabilized in 200 μL of 0.1% Triton-X in PBS for 10 min at room temperature. After washing, each pellet was resuspended in 100 μL of a saturation solution (PBS without calcium and magnesium containing 10% of goat serum) and incubated for 20 min on ice. Anti-Acetyl H3 (Lys 9) rabbit monoclonal antibody (Thermo Scientific, OH, USA) was added diluted 1:100 in the saturation solution. Samples were incubated for 1 h on ice. Primary antibody was removed and secondary FITC goat anti-rabbit IgG antibody (Millipore, MA, USA) was added (20 μg mL^{-1}) and incubated on ice in the dark for 45 min. Secondary antibody was removed and, prior to running on the FC500, cells were resuspended in 400 μL of PBS. About 10000 events were collected for all samples on FC500 using 488 nm laser excitation and analysed with CXP software (Bekmann Coulter). Mean fluorescence intensity (MFI) was obtained by histogram statistics and are provided to quantify the H3 acetylation.

Appendix A. Supplementary data

Supplementary data related to this article can be found at http://dx.doi.org/10.1016/j.ejmech.2014.11.012.

References

[1] L. Carion, C. Jacquard, O. Sainte-Catherine, S. Loiseau, D. Filippini, M.H. Hirlemann, J.N. Volle, D. Virieux, M. Lecouvey, J.L. Pirat, N. Bakalara, Oxaphosphinanes: new therapeutic perspectives for glioblastoma, J. Med. Chem. 55 (2012) 2196–2211.

[2] J.T. Huse, E.C. Holland, Targeting brain cancer: advances in the molecular pathology of malignant glioma and medulloblastoma, Nat. Rev. Cancer 10 (2010) 319–331.
[3] D.S. Bidros, M.A. Vogelbaum, Novel drug delivery strategies in neuro-oncology, Neurotherapeutics 6 (2009) 539–546.
[4] V. Megalizzi, C. Decaestecker, O. Debeir, S. Spiegl-Kreinecker, W. Berger, F. Lefranc, R.E. Kast, R. Kiss, Screening of anti-glioma effects induced by sigma-1 receptor ligands: potential new use for old anti-psychiatric medicines, Eur. J. Cancer 45 (2009) 2893–2905.
[5] R.E. Kast, Glioblastoma: looking at the currently marketed sigma-1 agonists and antagonists, Neoplasia 9 (2007) 689.
[6] I. Gil-Ad, B. Shtaif, Y. Levkovitz, M. Dayag, E. Zeldich, A. Weizman, Characterization of phenothiazine-induced apoptosis in neuroblastoma and glioma cell lines: clinical relevance and possible application for brain-derived tumors, J. Mol. Neurosci. 22 (2004) 189–198.
[7] V. Megalizzi, V. Mathieu, T. Mijatovic, P. Gailly, O. Debeir, N. De Neve, M. Van Damme, G. Bontempi, B. Haibe-Kains, C. Decaestecker, Y. Kondo, R. Kiss, F. Lefranc, 4-IBP, a sigma1 receptor agonist, decreases the migration of human cancer cells, including glioblastoma cells, in vitro and sensitizes them in vitro and in vivo to cytotoxic insults of proapoptotic and proautophagic drugs, Neoplasia 9 (2007) 358–369.
[8] A. van Waarde, K. Shiba, J.R. de Jong, K. Ishiwata, R.A. Dierckx, P.H. Elsinga, Rapid reduction of sigma1-receptor binding and 18F-FDG uptake in rat gliomas after in vivo treatment with doxorubicin, J. Nucl. Med. 48 (2007) 1320–1326.
[9] N.A. Colabufo, F. Berardi, M. Contino, M. Niso, C. Abate, R. Perrone, V. Tortorella, Antiproliferative and cytotoxic effects of some sigma(2) agonists and sigma(1) antagonists in tumour cell lines, Naunyn Schmiedebergs Arch. Pharmacol. 370 (2004) 106–113.
[10] F. Kratz, I.A. Muller, C. Ryppa, A. Warnecke, Prodrug strategies in anticancer chemotherapy, ChemMedChem 3 (2008) 20–53.
[11] A. Marrazzo, J. Fiorito, L. Zappala, O. Prezzavento, S. Ronsisvalle, L. Pasquinucci, G.M. Scoto, R. Bernardini, G. Ronsisvalle, Antiproliferative activity of phenylbutyrate ester of haloperidol metabolite II [(+/−)-MRJF4] in prostate cancer cells, Eur. J. Med. Chem. 46 (2011) 433–438.
[12] F. Lefranc, J. Brotchi, R. Kiss, Possible future issues in the treatment of glioblastomas: special emphasis on cell migration and the resistance of migrating glioblastoma cells to apoptosis, J. Clin. Oncol. 23 (2005) 2411–2422.
[13] D.N. Louis, H. Ohgaki, O.D. Wiestler, W.K. Cavenee, P.C. Burger, A. Jouvet, B.W. Scheithauer, P. Kleihues, The 2007 WHO classification of tumours of the central nervous system, Acta Neuropathol. 114 (2007) 97–109.
[14] C. Dell'Aversana, I. Lepore, L. Altucci, HDAC modulation and cell death in the clinic, Exp. Cell. Res. 318 (2012) 1229–1244.
[15] I. Okun, K.V. Balakin, S.E. Tkachenko, A.V. Ivachtchenko, Caspase activity modulators as anticancer agents, Anticancer Agents Med. Chem. 8 (2008) 322–341.
[16] J. Zhu, H. Wan, C.Q. Xue, T. Jiang, C. Qian, Y.Q. Zhang, Histone deacetylase 3 implicated in the pathogenesis of children glioma by promoting glioma cell proliferation and migration, Brain Res. 1520 (2013) 15–22.
[17] P. Jones, S. Altamura, R. De Francesco, O.G. Paz, O. Kinzel, G. Mesiti, E. Monteagudo, G. Pescatore, M. Rowley, M. Verdirame, C. Steinkuhler, A novel series of potent and selective ketone histone deacetylase inhibitors with antitumor activity in vivo, J. Med. Chem. 51 (2008) 2350–2353.
[18] T. Kouzarides, Histone acetylases and deacetylases in cell proliferation, Curr. Opin. Genet. Dev. 9 (1999) 40–48.
[19] J.C. Jaen, B.W. Caprathe, S. Priebe, L.D. Wise, Synthesis of the enantiomers of reduced haloperidol, Pharm. Res. 8 (1991) 1002–1005.
[20] S. Carrara, V. Reali, P. Misiano, G. Dondio, C. Bigogno, Evaluation of in vitro brain penetration: optimized PAMPA and MDCKII-MDR1 assay comparison, Int. J. Pharm. 345 (2007) 125–133.
[21] M. Malakoutikhah, M. Teixido, E. Giralt, Toward an optimal blood-brain barrier shuttle by synthesis and evaluation of peptide libraries, J. Med. Chem. 51 (2008) 4881–4889.
[22] H.S. Kim, M.S. Song, S. Yumkham, J.H. Choi, T. Lee, J. Kwon, S.J. Lee, J.I. Kim, K.W. Lee, P.L. Han, S.W. Shin, J.H. Baik, Y.S. Kim, S.H. Ryu, P.G. Suh, Identification of a new functional target of haloperidol metabolite: implications for a receptor-independent role of 3-(4-fluorobenzoyl) propionic acid, J. Neurochem. 99 (2006) 458–469.
[23] M. Kansy, F. Senner, K. Gubernator, Physicochemical high throughput screening: parallel artificial membrane permeation assay in the description of passive absorption processes, J. Med. Chem. 41 (1998) 1007–1010.
[24] H. Fischer, M. Kansy, A. Avdeef, F. Senner, Permeation of permanently positive charged molecules through artificial membranes–influence of physico-chemical properties, Eur. J. Pharm. Sci. 31 (2007) 32–42.
[25] K.M. Fabio, C.D. Guillon, S.F. Lu, N.D. Heindel, M.J. Brownstein, C.J. Lacey, C. Garippa, N.G. Simon, Pharmacokinetics and metabolism of SRX246: a potent and selective vasopressin 1a antagonist, J. Pharm. Sci. 102 (2013) 2033–2043.
[26] P. Sozio, L.S. Cerasa, S. Laserra, I. Cacciatore, C. Cornacchia, E.S. Di Filippo, S. Fulle, A. Fontana, A. Di Crescenzo, M. Grilli, M. Marchi, A. Di Stefano, Memantine-sulfur containing antioxidant conjugates as potential prodrugs to improve the treatment of Alzheimer's disease, Eur. J. Pharm. Sci. 49 (2013) 187–198.
[27] A. Marrazzo, E.J. Cobos, C. Parenti, G. Arico, G. Marrazzo, S. Ronsisvalle, L. Pasquinucci, O. Prezzavento, N.A. Coabufo, M. Contino, L.G. Gonzalez, G.M. Scoto, G. Ronsisvalle, Novel potent and selective sigma ligands: evaluation of their agonist and antagonist properties, J. Med. Chem. 54 (2011) 3669–3673.
[28] J.C. Jaen, B.W. Caprathe, T.A. Pugsley, L.D. Wise, H. Akunne, Evaluation of the effects of the enantiomers of reduced haloperidol, azaperol, and related 4-amino-1-arylbutanols on dopamine and sigma-receptors, J. Med. Chem. 36 (1993) 3929–3936.
[29] J.M. Walker, W.D. Bowen, F.O. Walker, R.R. Matsumoto, B. Decosta, K.C. Rice, Sigma-receptors - biology and function, Pharmacol. Rev. 42 (1990) 355–402.
[30] R.B. Rothman, A. Reid, A. Mahboubi, C.H. Kim, B.R. Decosta, A.E. Jacobson, K.C. Rice, Labeling by [H-3] 1,3-di(2-tolyl)guanidine of 2 high-affinity binding-sites in guinea-pig brain - evidence for allosteric regulation by calcium-channel antagonists and pseudoallosteric modulation by sigma ligands, Mol. Pharmacol. 39 (1991) 222–232.
[31] R. Paul, S. Lavastre, D. Floutard, R. Floutard, X. Canat, P. Casellas, G. Lefur, J.C. Breliere, Allosteric modulation of peripheral sigma-binding sites by a new selective ligand - Sr-31747, J. Neuroimmunol. 52 (1994) 183–192.
[32] G. Ronsisvalle, A. Marrazzo, O. Prezzavento, L. Pasquinucci, B. Falcucci, R. Di Toro, S. Spampinato, Substituted 1-phenyl-2-cyclopropylmethylamines with high affinity and selectivity for sigma sites, Bioorg. Med. Chem. 8 (2000) 1503–1513.
[33] A. Marrazzo, O. Prezzavento, M.S. Pappalardo, E. Bousquet, M. Iadanza, V.W. Pike, G. Ronsisvalle, Synthesis of (+)- and (-)-cis-2-[(1-adamantylamino)-methyl]-1-phenylcyclopropane derivatives as high affinity probes for sigma(1) and sigma(2) binding sites, Farmaco 57 (2002) 45–53.
[34] E.J. Cobos, E. del Pozo, J.M. Baeyens, Irreversible blockade of sigma-1 receptors by haloperidol and its metabolites in guinea pig brain and SH-SY5Y human neuroblastoma cells, J. Neurochem. 102 (2007) 812–825.
[35] C.C. Ooi, N.M. Good, D.B. Williams, T. Lewanowitsch, L.J. Cosgrove, T.J. Lockett, R.J. Head, Structure-activity relationship of butyrate analogues on apoptosis, proliferation and histone deacetylase activity in HCT-116 human colorectal cancer cells, Clin. Exp. Pharmacol. Physiol. 37 (2010) 905–911.
[36] L. Montenegro, C. Carbone, C. Maniscalco, D. Lambusta, G. Nicolosi, C.A. Ventura, G. Puglisi, In vitro evaluation of quercetin-3-O-acyl esters as topical prodrugs, Int. J. Pharm. 336 (2007) 257–262.
[37] P. Sozio, E. D'Aurizio, A. Iannitelli, A. Cataldi, S. Zara, F. Cantalamessa, C. Nasuti, A. Di Stefano, Ibuprofen and lipoic acid diamides as potential codrugs with neuroprotective activity, Arch. Pharm. (Weinheim) 343 (2010) 133–142.
[38] I. Cacciatore, L. Baldassarre, E. Fornasari, C. Cornacchia, A. Di Stefano, P. Sozio, L.S. Cerasa, A. Fontana, S. Fulle, E.S. Di Filippo, R.M. La Rovere, F. Pinnen, (R)-alpha-lipoyl-glycyl-l-prolyl-L-glutamyl dimethyl ester codrug as a multifunctional agent with potential neuroprotective activities, ChemMedChem 7 (2012) 2021–2029.
[39] T. Mennini, P. Bernasconi, M.G. Fiori, Neurotoxicity of nonionic low-osmolar contrast-media - a receptor-binding study, Invest. Radiol. 28 (1993) 821–827.
[40] S. Ronzoni, M. Faretta, M. Ballarini, P. Pelicci, S. Minucci, New method to detect histone acetylation levels by flow cytometry, Cytom. A 66A (2005) 52–61.